EVS30 Symposium
Stuttgart, Germany, October 9 - 11, 2017

Power Management of Wireless In-Wheel Motor with Dynamic-Wireless Power Transfer

Takuma Takeuchi[1], Takehiro Imura[2], Hiroshi Fujimoto[3], Yoichi Hori[4]
[1−4]*The University of Tokyo, 5-1-5,Kashiwanoha, Kashiwa, Chiba, 277-8561, Japan,* [1] *takeuchi15@hflab.k.u-tokyo.ac.jp*

Abstract

In-Wheel Motor (IWM) which is a driving system of Electric Vehicles (EVs) is effective for improving driving stability of vehicle and reducing vehicle weight. However, IWM has not been put in practical use because of a possibility of power lines disconnection. Therefore, we have proposed Wireless In-Wheel Motor (W-IWM) in which Wireless Power Transfer (WPT) is used to remove these lines and to enhance practicability of IWM. Moreover, we have proposed the advanced system of W-IWM which has Lithium-ion Capacitor (LiC) and circuit for Dynamic-Wireless Power Transfer (D-WPT) on its wheel-side. In this paper, power management method of this system is proposed. By applying this control method, efficiency of regenerative breaking can be improved. Moreover, dynamic-wireless power transfer from a road-side infrastructure can be achieved on the wheel-side. The proposed method is verified by simulations and experiments including actual vehicle driving test.

Keywords: Wireless In-Wheel Motor, Wireless Power Transfer, Lithium-ion Capacitor, Power management, State of Charge, Dynamic-Wireless Power Transfer

1 INTRODUCTION

Electric Vehicles (EVs) have been gathering a great deal of public attention from the perspective of environmental performance. However, due to a limited battery capacity, EVs has been only able for short distance. To deal with this problem, a number of researches have been done on effective motor driving for EVs [1] or driving range extension by vehicle motion control using In-Wheel Motor (IWM) [**?**]. IWM is one of the drive systems which equipped motors in its wheels. Owing to the independent toque control of each wheel, IWM can achieve high vehicle stability and long driving range [3]. Nevertheless, IWM has not been put to practical use due to the risk of power lines disconnection mainly caused by continuous displacement between wheels and chassis while driving.

Therefore, we have proposed Wireless In-Wheel Motor (W-IWM) to solve this problem radically and to make IWM more practical by using Wireless Power Transfer (WPT) via magnetic resonance coupling [4, 5, 6]. We have already succeeded in driving an experimental vehicle with the first trial unit of W-IWM. The first trial unit of W-IWM achieves transmitting 3.3 kW/wheel and 89 % DC to DC efficiency from the chassis-side to the wheel-side via WPT [7]. For more improvement of practicability, high power and further effective operation are expected.

Accordingly, the second trial unit of W-IWM (W-IWM2), which has Lithium-ion Capacitor (LiC) on the wheel-side for higher output and more efficient operation is developed. W-IWM2 enables more efficient regenerative breaking from wheel to LiC because the regenerative power goes through less number of converters compared with W-IWM. Additionally, circuit for receiving Dynamic-Wireless Power Transfer (D-WPT) from a road-side facility is also added on the wheel-side for more range extension.

As a result, W-IWM2 has multiple power sources (WPT from the chassis-side, LiC and D-WPT from the road-side) [9, 10] on the wheel-side. Therefore, power-flow control of these power sources is required

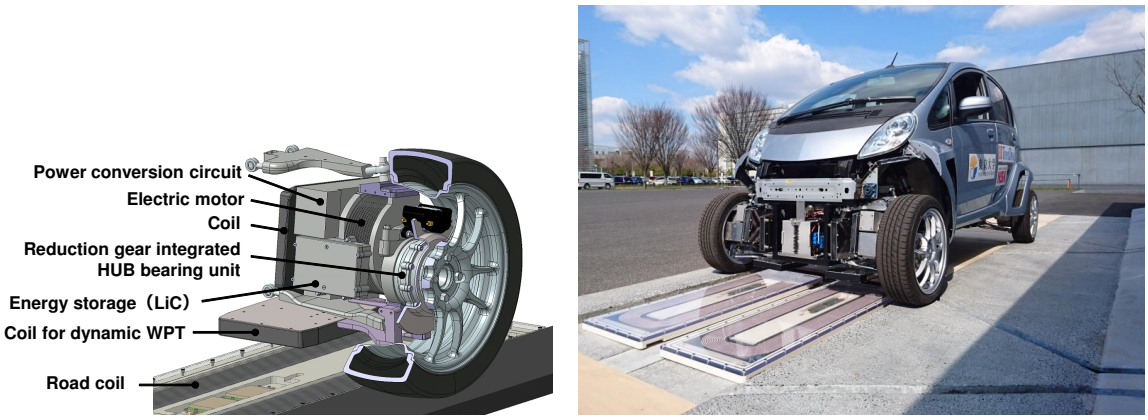

(a) The second trial unit of W-IWM (b) Experimental vehicle equipped with W-IWM2

Figure 1: The second trial unit of W-IWM and experimental vehicle.

for stable motor driving [8]. When too much/insufficient power are supplied from these power sources to the motor, the wheel-side DC-link voltage goes up/down. Moreover, energy generated by regenerative brake should be charged to LiC for operation efficiency improvement. Therefore, power management on the wheel-side is necessary for W-IWM2.

In this paper, we propose power management method of this system by DC-link voltage feedback control by the wheel-side DC/DC converter and State of Charge (SOC) control of LiC. Applying this control to W-IWM2, a voltage of LiC is stabilized and output/input power of LiC can be decided properly according to a load power (power of the PMSM and three-phase PWM inverter). The proposed power management method is verified by simulations and experiments including the actual vehicle driving test.

2 WIRELESS IN-WHEEL MOTOR2 (W-IWM2)

2.1 Concept

These days, a lot of researches on D-WPT for EVs's driving range extension are reported. These researches are mainly discusses on D-WPT from a road-side infrastructure to an on board battery. On the other hand, W-IWM2 proposed D-WPT from the road-side infrastructure to IWM directly. D-WPT for IWM can achieve many advantage as follows;

1) D-WPT efficiency improvement

2) Receiving coil can be placed on minimum ground clearance and coil gap does not change

3) Transmission power from a road-side coil can be reduced

Because transmission power does not go thought the on board battery, transmission efficiency from a road-side inverter to an IWM can be improved. Conventional receiving coil for D-WPT is placed on the bottom of a vehicle and coils gap between a road-side coil and vehicle-side coil is changed by dynamics of the vehicle. On the other hand, D-WPT for IWM can place the receiving coil on IWM with minimum ground clearance and gap does not change. Therefore, D-WPT for IWM can realize efficient and stable D-WPT. Moreover, receiving coils for D-WPT can be placed on each wheel. This means that required receiving power for the vehicle from the road-side can be divided by the numbers of receiving coils. Additionally, a road-side coil can be separated into two coils for right and left wheel each. Therefore, considering the vehicle equipped with W-IWM2 on all wheels, transmission power from a road-side coil can be reduced to a quarter of the conventional D-WPT.

2.2 Construction

Fig. 1 shows the second trial unit and the experimental vehicle. This system has its drive-train, motor and reduction gear integrated HUB unit, on the wheel-side. Moreover, this system has energy storage (LiC) and receiving coils for the chassis-side and the road-side on the wheel-side. As a trial setup, this vehicle is equipped with W-IWM2 on its front two-wheels. The road-side infrastructure has coils in parallel for right and left wheels. Each coil on the road-side has an inverter to generate 85 kHz resonant

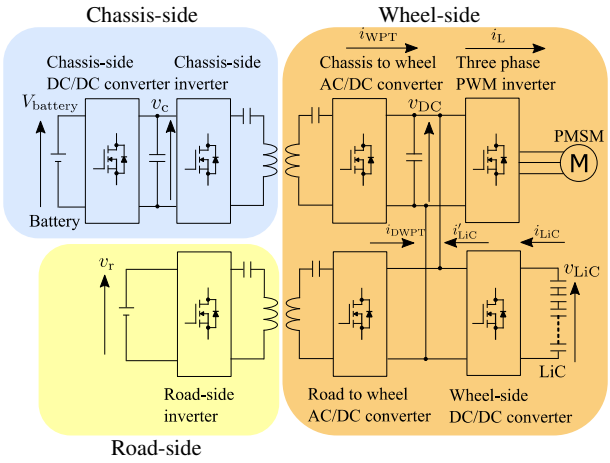

Figure 2: System configuration of W-IWM2.

current and detect a vehicle driving on the coil. Maximum output of a road-side coil is designed as 9 kw. When W-IWM2 is installed for all the four-wheels of the vehicle, the read-side can output 36 kW for the vehicle at most.

Fig. 2 shows a system of W-IWM2, where v_{DC} is the wheel-side DC-link voltage, v_{LiC} is voltage of LiC, v_{r} is an input DC voltage of a road-side inverter, i_{L} is DC input current of load (PMSM and three-phase PWM inverter), i_{WPT} is output DC current of the chassis to wheel AC/DC converter, i_{LiC} is output current of LiC, i'_{LiC} is output current of the wheel-side DC/DC converter and i_{DWPT} is output DC current of the road to wheel AC/DC converter. In this system, LiC is connected to the DC-link through the wheel-side DC/DC converter, and a receiving coil for D-WPT from the road-side is also connected to the DC-link through an AC/DC converter.

Whereas W-IWM regenerates regenerative braking power to the chassis-side via WPT, W-IWM2 can regenerate wheel power to LiC via the wheel-side DC/DC converter. Therefore, regenerative power goes through a small number of converters compared to W-IWM. DC to DC efficiency of regenerative braking is expected to be improved from 89 % to 96 %. Additionally, D-WPT from the road-side infrastructure can be applied to W-IWM2. Thus more range extension can be expected.

3 POWER MANAGEMENT METHOD FOR W-IWM2

This chapter describes the proposed power management method for W-IWM2.

3.1 Overview of the control method

Because of constant power load characteristic of motor, DC-link voltage of this system need to be stabilized. When the output and input power of DC-link are balanced, the DC-link voltage will be constant. However, power from multiple power-sources come and go to the DC-link intermittently. This makes the DC-link voltage unstable. Therefore, the objective of this control method is to manage the power-flow among these power-sources adequately for stabilizing the DC-link voltage. Furthermore, SOC of LiC is also need to be controlled. Therefore, SOC control of LiC is required to be realized simultaneously.

Schematics of operation modes of W-IWM2 with this proposed method is shown in Fig. 3. Fig. 3(a) shows power-flow in case of receiving D-WPT. Received power from the road-side is used by driving the IWM. Surplus power is charged LiC and is regenerated to the chassis-side. Fig. 3(b) shows power-flow in case of driving the IWM without D-WPT. The IWM is mainly driven by WPT from chassis-side. When the IWM requires large power for acceleration or LiC has high SOC value because of regenerative braking or D-WPT, LiC supply the energy for IWM. Fig. 3(c) shows power-flow in case of the IWM operates in regenerative breaking mode. Regenerative power is charged to LiC and is transmitted to the chassis-side if the SOC of LiC is exceed objective value.

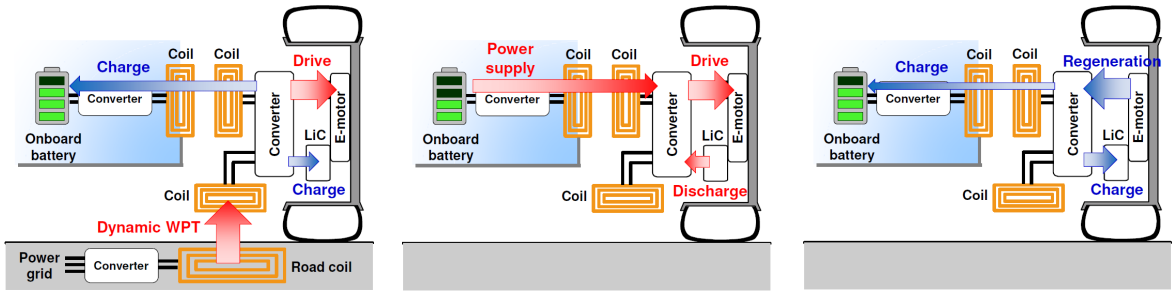

(a) With D-WPT (b) Without D-WPT (c) Electrical breaking regeneration

Figure 3: Operation modes of W-IWM2 with power management method.

3.2 DC-link Voltage control

The wheel-side DC/DC converter controls the wheel-side DC-link voltage v_{DC} by voltage feedback control. By means of the voltage feedback control, power of LiC P_{LiC} is decided passively according to a power-flow transition. This means that eq. (1) is achieved.

$$
\begin{aligned}
P_{\mathrm{L}} &= P_{\mathrm{WPT}} + P_{\mathrm{LiC}} + P_{\mathrm{DWPT}} && (1)\\
P_{\mathrm{L}} &= i_{\mathrm{L}} v_{\mathrm{DC}} && (2)\\
P_{\mathrm{WPT}} &= i_{\mathrm{WPT}} v_{\mathrm{DC}} && (3)\\
P_{\mathrm{LiC}} &= i'_{\mathrm{LiC}} v_{\mathrm{DC}} && (4)\\
P_{\mathrm{DWPT}} &= i_{\mathrm{DWPT}} v_{\mathrm{DC}} && (5)
\end{aligned}
$$

Where P_{L} is load power, P_{WPT} is transmission power via WPT from the chassis-side and P_{DWPT} is received power from the road-side.

The circuit model of the wheel-side DC/DC converter is shown in Fig. 4, where r is equivalent series resistance of LiC and reactor, L is reactance of DC/DC converter and C is capacitance of the wheel-side DC-link smoothing capacitor. In this model, PMSM and three-phase PWM inverter are modeled by current source.

To analyze this circuit and design voltage feedback controller, the state-space averaging method is applied. In this paper, because switching of this half bridge is reciprocal, this model works in continuous current mode only. Since the system includes nonlinearity, linearization on its equilibrium point and minute variations analysis are conducted. Subsequently, the transfer function ΔP_{v} from $\Delta d'(s)$ to $\Delta v_{\mathrm{DC}}(s)$ is expressed as follows:

$$
\begin{aligned}
\Delta P_{\mathrm{v}} &= \frac{\Delta v_{\mathrm{DC}}(s)}{\Delta d'(s)} = \frac{b_{\mathrm{p1}} s + b_{\mathrm{p0}}}{s^2 + a_{\mathrm{p1}} s + a_{\mathrm{p0}}} && (6)\\
a_{\mathrm{p1}} &= \frac{r}{L}, a_{\mathrm{p0}} = -\frac{D'}{LC}\\
b_{\mathrm{p1}} &= \frac{I_{\mathrm{LiC}}}{C}, b_{\mathrm{p0}} = \frac{r I_{\mathrm{LiC}} - D' V_{\mathrm{DC}}}{LC},
\end{aligned}
$$

where $\Delta d'(s)$ is a minute variation of the duty ration of the upper arm switch and $\Delta v_{\mathrm{DC}}(s)$ is a minute variation of the wheel-side DC-link voltage. Based on this transfer function, the PID controller such that closed-loop characteristic has quadrupole on real axis is designed and is discretized with Tustin conversion.

3.3 SOC control of LiC

The chassis to wheel AC/DC converter controls WPT between the chassis-side and the wheel-side P_{WPT} by changing its voltage duty ratio and phase difference. By means of P_{WPT} control of the wheel-side AC/DC converter, P_{LiC} which is decided by v_{DC} feedback control can be controlled indirectly as shown in eq. (1).

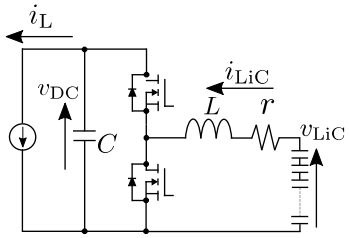

Figure 4: Circuit model of wheel-side DC/DC converter.

Compared to v_{DC} feedback control which is compensating power balance of the system in short time, SOC control of LiC is controlling SOC of LiC according to driving pattern of the vehicle in relatively longer time. In other word, in the case of the vehicle requiring acceleration/deceleration or high responsiveness, LiC can be used initiatively. On the other hand, under the cruising condition, the chassis-side battery is used initiatively. This utilization ration can be design by band wise of controllers for each control.

Fig. 5 shows concept of phase shift rectification which applied to the chassis to wheel AC/DC converter to control P_{WPT}, where i_{cw} is input current of the chassis to wheel AC/DC converter and v_{cw} is input voltage of the chassis to wheel AC/DC converter. Here we defined the voltage duty ratio of phase shift rectification α_{ps} as follow;

$$\alpha_{\mathrm{ps}} = \frac{T_{\mathrm{r}}}{T}\,(-1 \leq \alpha_{\mathrm{ps}} \leq 1). \tag{7}$$

In addition, the sign of α_{ps} shows the direction of WPT. Pulse means the chassis-side battery powers the IWM, and minus means the power regenerated to the chassis-side battery from the wheel-side. By changing α_{ps}, average output current of the chassis to wheel AC/DC converter $\bar{i}_{\mathrm{WPT}}$ can be controlled. Moreover, the direction of WPT can be reversed by shifting the phase difference between i_{cw} to v_{cw}. By shifting the phase difference from 0 rad to π rad, the direction of WPT can be reversed. Assuming that i_{cw} is sinusoidal wave, relation between $\bar{i}_{\mathrm{WPT}}$ to α_{cw} is calculated as follow[11];

$$\begin{aligned}\bar{i}_{\mathrm{WPT}} &= \frac{1}{\pi}\int_{\frac{\pi}{2}-\frac{\pi}{2}\alpha_{\mathrm{ps}}}^{\frac{\pi}{2}+\frac{\pi}{2}\alpha_{\mathrm{ps}}} i_{\mathrm{WPT}}\sin\theta d\theta \\ &= \frac{2}{\pi} i_{\mathrm{WPT}}\sin\frac{\pi\alpha_{\mathrm{ps}}}{2}.\end{aligned} \tag{8}$$

Generating α_{ps} from v_{LiC} makes SOC control of LiC possible. Assuming that the v_{DC} control by the wheel-side DC/DC converter keeps v_{DC} constant, eq. (9) is derived from eq. (1) and the wheel-side circuit model can be expressed by Fig. 6.

$$i_{\mathrm{L}} = i_{\mathrm{WPT}} + i'_{\mathrm{LiC}} + i_{\mathrm{DWPT}} \tag{9}$$

Assuming that a loss of the wheel-side DC/DC converter is small enough, formula eq. (10) is derived.

$$i'_{\mathrm{LiC}} v_{\mathrm{DC}} = i_{\mathrm{LiC}} v_{\mathrm{LiC}} \tag{10}$$

Furthermore, a relation expression of a LiC current i_{LiC} and voltage v_{LiC} can be expressed as

$$i_{\mathrm{LiC}} = -C_{\mathrm{LiC}}\frac{dv_{\mathrm{LiC}}}{dt}. \tag{11}$$

Therefore, from eq. (9), eq. (10) and eq. (11), the following equation is derived.

$$i_{\mathrm{WPT}} = (C\frac{d}{dt} + \frac{1}{R_{\mathrm{L}}})v_{\mathrm{DC}} + \frac{C_{\mathrm{LiC}}}{v_{\mathrm{DC}}} v_{\mathrm{LiC}}\frac{dv_{\mathrm{LiC}}}{dt} - i_{\mathrm{DWPT}} \tag{12}$$

By linearizing the formula above using Taylor expansion, a transfer function from Δi_{WPT} to Δv_{LiC} can be expressed as,

$$\Delta P_{\mathrm{SOC}} = \frac{\Delta v_{\mathrm{LiC}}}{\Delta i_{\mathrm{WPT}}} = \frac{V_{\mathrm{DC}}}{2C_{\mathrm{LiC}}V_{\mathrm{LiC}}s}. \tag{13}$$

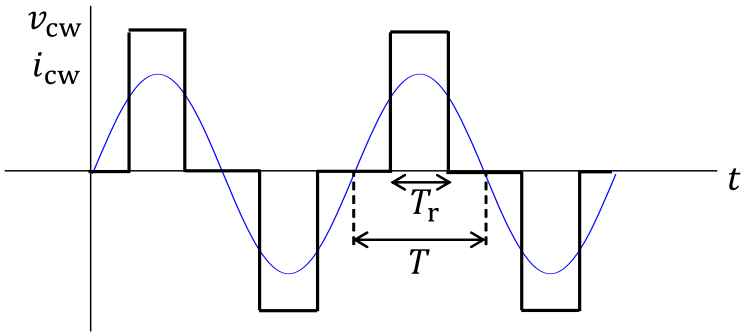

Figure 5: Phase-shift rectification on the chassis to wheel AC/DC converter.

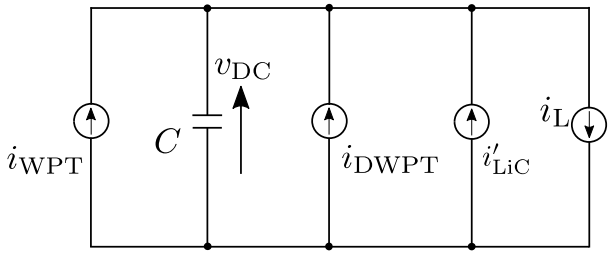

Figure 6: Circuit model of the wheel-side on W-IWM2.

Consequently, the PI controller for the plant model expressed by eq. (8) and eq. (13) such that closed-lope poles have dual pole p_{PI} on real axis. Finally, this PI controller is discretized with Tustin conversion.
The block diagram of the power management method shown in Fig. 7 can be expressed by the combination of these two control mentioned above.

4 SIMULATIONS

We performed simulations on the proposed control method using MATLAB Simulink Simpower Systems.Simulation conditions are shown in Tab. 1. In these simulation, rectification method applied to the chassis to wheel AC/DC converter is two-mode control[8].

4.1 Load power fluctuation

We conducted a simulation on stepwise load power fluctuations. For simplicity, we excluded D-WPT from the road-side in this simulation. Here, LiC powers/regenerates to compensate the wheel-side power-flow promptly. Therefore, SOC of LiC changes according to output/input power of LiC. Subsequently, P_{WPT} is controlled to make SOC of LiC follow the command value automatically.
Fig. 8 shows the simulation result in case of load power fluctuation. Fig. 8(a) shows power of each power source on the wheel-side. P_{LiC} tracks stepwise changes of P_L rapidly, subsequently P_{WPT} is controlled to charge/discharge LiC automatically. Fig. 8(b) shows that the v_{DC} control of the wheel-side DC/DC converter can suppress v_{DC} variations caused by stepwise transitions of P_L. Fig. 8(c) shows that SOC of LiC tracks the command value before and after the load change.
Consequently, the proposed control method in the case of stepwise load fluctuations can is verified.

4.2 Power-flow change with Dynamic Wireless Power Transfer

We conducted a simulation on power-flow change with D-WPT. When the load powers at 6.0 kW, the wheel-side receiving coil for D-WPT moves at 80 km/h and receives transmitted power from the road-side.
Fig. 9(a) shows the experimental result of power-flow change with D-WPT. Fig. 9(a) shows power of each power source on the wheel-side. The load uses receiving power from D-WPT, then excess portion charge LiC. While receiving D-WPT from road-side, WPT from chassis-side stop according to the rise

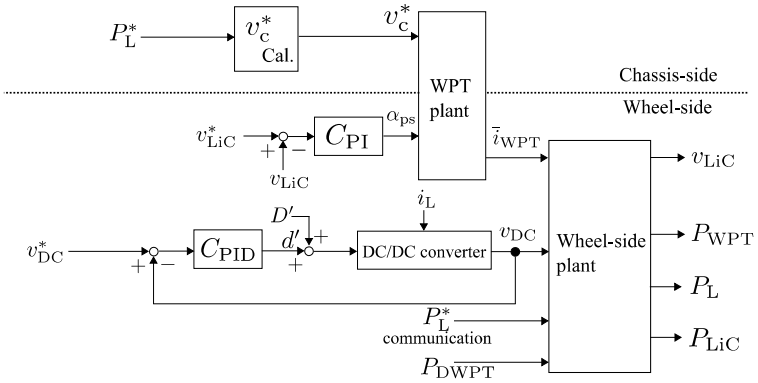

Figure 7: Block diagram of W-IWM2.

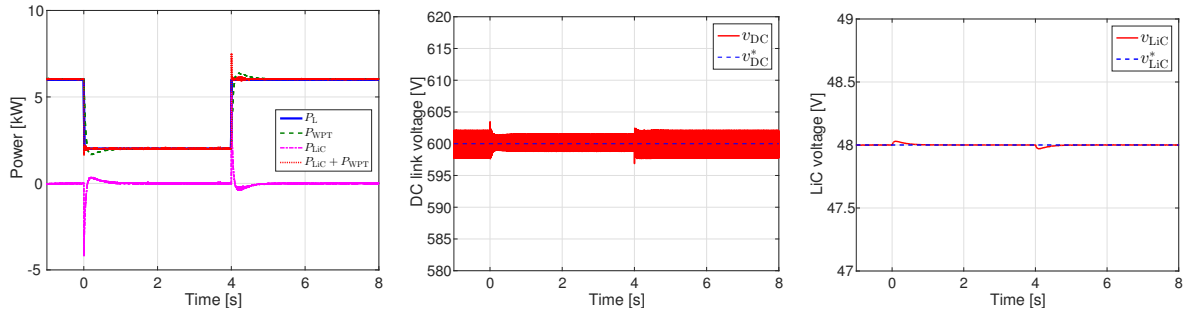

(a) Power (b) DC-link voltage v_{DC} (c) LiC voltage v_{LiC}

Figure 8: Simulation results of load power increament.

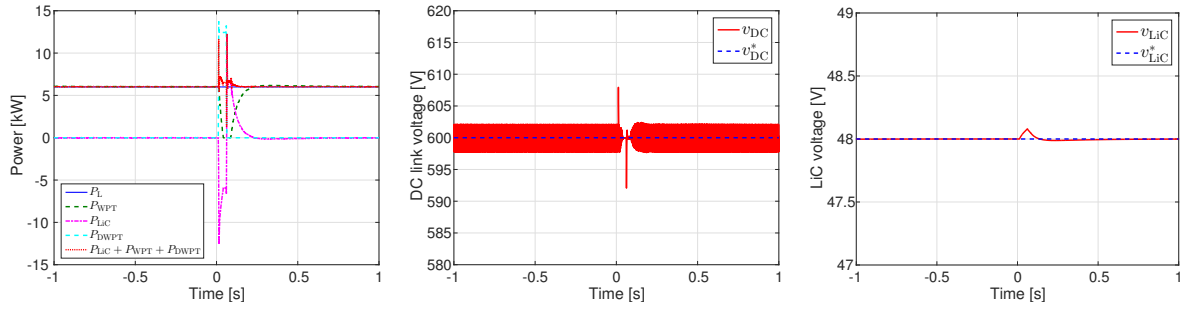

(a) Power (b) DC-link voltage v_{DC} (c) LiC voltage v_{LiC}

Figure 9: Simulation results of power management with D-WPT.

of SOC of LiC. Fig. 9(b) shows that the v_{DC} control of the wheel-side DC/DC converter can suppress v_{DC} variations caused by D-WPT. Fig. 9(c) shows that SC is charged by D-WPT and charged power is used by the load.

Consequently, we verified that the power management in the case of receiving D-WPT from road-side.

5 EXPERIMENTS

We conducted same experiments as simulations using the small power experimental setup shown in Fig. 10(a). Based on these experiments, actual vehicle test is also conducted.

Table 1: Simulation and experimental parameters.

	Sim.	Exp.	W-IWM2
Resonance frequency	85 kHz	85 kHz	85 kHz
Switching frequency of DC/DC converter	40 kHz	40 kHz	85 kHz
Chassis-side converter output voltage v_{c}	578 V	300 V	500 V
DC-link voltage reference v^*_{DC}	487 V	200 V	500V
Maximum output of load	12.0 kW	1.2 kW	12.0 kW
LiC capacitance	93.8 F	95.8 F	125 F
LiC voltage reference v^*_{LiC}	48 V	50 V	38 V
chassis-side coil resistance R_{c}	400.0 mΩ	558.1 mΩ	242.0 mΩ
chassis-side coil inductance L_{c}	270.0 μH	269.7μH	259.9μH
Chassis to wheel coil resistance R_{cw}	300.0 mΩ	361.8 mΩ	242.0 mΩ
Chassis to wheel coil inductance L_{cw}	250.0 μH	224.5μH	259.9μH
Road-side coil resistance R_{r}	400.0 mΩ	867.1 mΩ	342.5 mΩ
Road-side coil inductance L_{r}	450.0 μH	292.0μH	429.0μH
Road to wheel coil resistance R_{rw}	300.0 mΩ	361.8 mΩ	383.3 mΩ
Road to wheel coil inductance L_{rw}	250.0 μH	223.9μH	377.7μH
Chassis - wheel coils gap	100 mm	100 mm	100 mm
Road - wheel coils gap	100 mm	100 mm	100 mm
Chassis to wheel coils mutual inductance L_{mcw}	52.0 μH	51.67 μH	60.1 μH
Road to wheel coils mutual inductance L_{mrw}	35.0 μH	34.51 μH	37.00 μH
DC-link capacitance C	2200 μF	2145 μF	1100 μF
Inductance of DC/DC converter L	60.8 μH	60.8 μH	60.8 μH
ESR of inductor and LiC r	31.4 mΩ	41.0 mΩ	41.0 mΩ

5.1 Experimental setup

Fig. 10(c) shows a circuit diagram of a small power experimental setup. The rectification method applied to the chassis to wheel AC/DC converter of this setup is two-mode control[8]. The bench test equipment is shown Fig. 10(b). This test bench can simulate driving motion of the wheel-side coil for D-WPT. The wheel-side coil for D-WPT moves toward the road-side coil at 18 km/h, and receives power transmitted from the road-side coil. To simplify the setup, a regenerative DC power supply (pCUBE MWBFP3-1250-J02 : Myway puls) replaces the load. A DC power supply (PU300-5 : TEXIO) replaces the battery and DC/DC converter on the chassis-side. The road-side inverter detects the motion of the wheel-side coil for D-WPT by sensorless vehicle detection method for D-WPT[12].

The experimental results are sampled at 20×10^{-6} sec. We filtered results of power by moving average with a window whose size is 2,000 to reduce v_{DC} and current ripple caused by two mode control of the wheel-side AC/DC converter. We applied 1 kHz primary low pass filter on the load current i_{L}, the current of LiC i_{LiC}, and the output current of the chassis to wheel AC/DC converter i_{WPT}.

5.2 Load power fluctuations

We conducted an experiment on stepwise load power fluctuations. Here we excluded D-WPT from the road-side for simplicity.

Fig. 11 shows the experimental results of load power fluctuations. Fig. 11(a) shows power of each power source on the wheel-side. We can confirm that P_{LiC} tracks stepwise changes of P_{L} to compensate wheel-side power-flow rapidly. Subsequently, P_{WPT} changes to make voltage of LiC tracking a command value v^*_{LiC} automatically. Because of the maximum transmitting power of the experimental setup is smaller than simulation, response of P_{WPT} is slower than the simulation result. Fig. 11(b) shows that the v_{DC} control of the wheel-side DC/DC converter can control v_{DC} changes caused by stepwise transitions of P_{L}. Fig. 11(c) shows that SOC of LiC tracks the command value before and after the load change.

Consequently, we verified that the power management in the case of stepwise load power fluctuations.

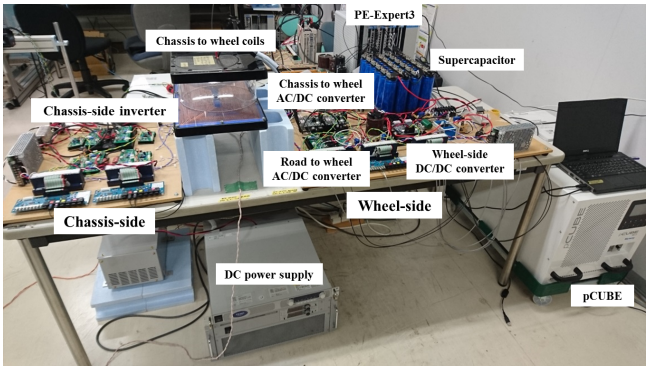

(a) Experimental setup

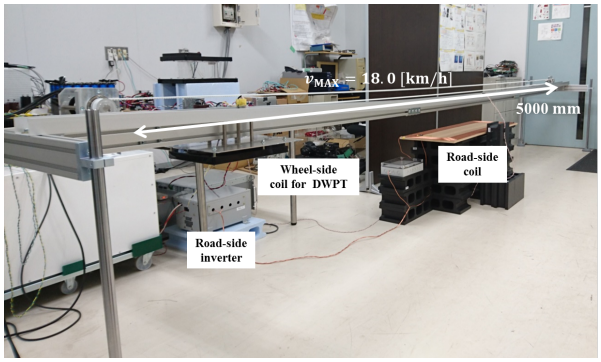

(b) Experimental setup for Dynamic-Wireless Power Transfer

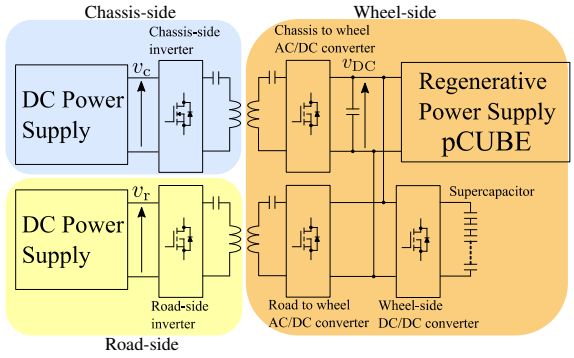

(c) Experimental circuit

Figure 10: Experimental setup.

5.3 Power-flow change with Dynamic-Wireless Power Transfer

We conducted an experiment on power-flow change with D-WPT. When the load powers at 1.0 kW, the wheel-side receiving coil for D-WPT moves at 18 km/h and receives transmitted power from the road-side.

Fig. 12 shows the experimental result of power-flow change with D-WPT. Fig. 12(a) shows power of each power source on the wheel-side. While receiving D-WPT from road-side, WPT from chassis-side stop automatically. Moreover, the load uses power of D-WPT, then excess portion charge SC. Fig. 12(b) shows that the v_{DC} control of the wheel-side DC/DC converter can suppress v_{DC} variations caused by D-WPT. Fig. 12(c) shows that SC is charged by D-WPT and charged power is used by the load. Therefore we can confirm that the power management is established.

Consequently, we verified that the power management in the case of receiving D-WPT from road-side.

5.4 Actual vehicle test with D-WPT

We conducted an experiment on D-WPT using the experimental vehicle with W-IWM2 on its front two-wheels and the road-side equipment shown in Fig. 1(b). The road-side has three coils in line at the interval of 1.6 m for right wheel. Road-side inverters detected the The torque value was generated by a driver using the acceleration pedal. The reference value of the DC-link voltage v^*_{DC} and the voltage of LiC v^*_{LiC} were set 500 V and 38 V respectively. The input DC voltage of the road-side inverter v_{r} is 200 V.

Fig. 13 shows the experimental result of actual vehicle test. Fig. 13(a) shows the torque value inputted to the right wheel. Fig. 13(b) shows the vehicle velocity. Fig. 13(d) shows RMS value of i_{rw}. we can confirm that W-IWM2 receives power from the road-side three times. Fig. 13(c) shows the DC-link voltage of the right wheel. Though there are voltage fluctuation caused by D-WPT, v_{DC} feedback control suppresses it. Fig. 13(e) shows i_{L} of the right wheel. Minus current means that LiC is charged by D-WPT. Passing the each coils on the road, LiC discharges its charged energy and powers the IWM automatically. This is because the SOC of LiC is stabilized by the power management method. Fig. 13(f) shows current on the second road-side coil. Spiking current before and after transmission is caused by

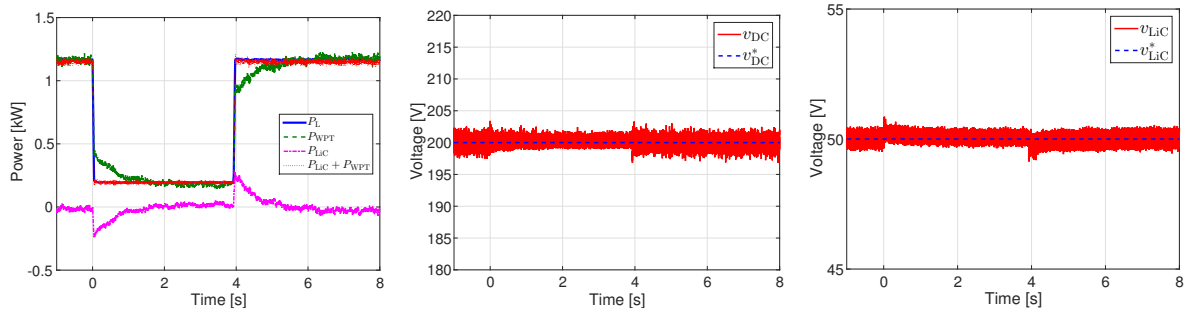

(a) Power (b) DC-link voltage v_{DC} (c) SC voltage v_{LiC}

Figure 11: Experimental results of load fluctuations.

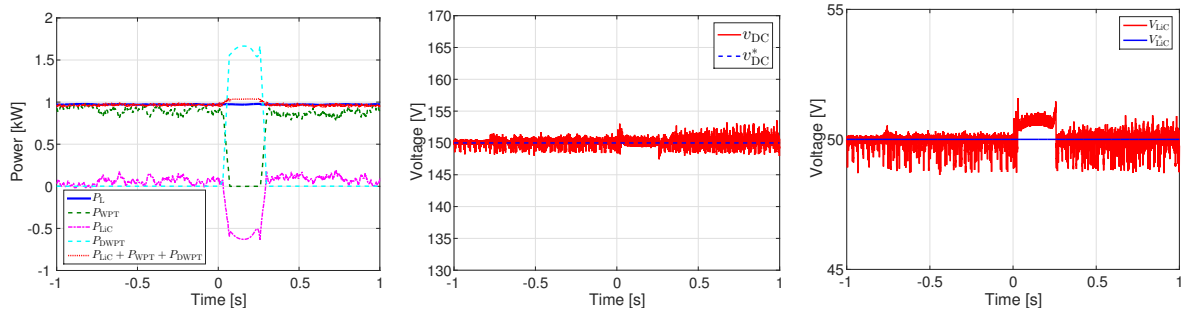

(a) Power (b) DC-link voltage v_{DC} (c) SC voltage v_{LiC}

Figure 12: Experimental results of power management with D-WPT.

the sensorless vehicle detection[12]. Power consumption of this vehicle detection is about 70 W, and transmission power from a road-side coil is about 3.8 kW.

We also conducted efficiency measurement on WPT from the road-side to the wheel-side in static. To adjust load condition, a regenerative DC power supply (pCUBE MWBFP3-1250-J02 : Myway puls) was connected to the DC-link instead of load. Tab. 2 shows result of the measurement. We confirmed that the system achieved high DC to DC(the road-side DC input to the wheel-side DC-link output) transmission efficiency.

From the result of actual vehicle driving test, we confirmed that the proposed power management method and D-WPT for W-IWM2 are realized.

6 CONCLUSION

In this research, power management method of the advanced system of W-IWM is proposed. By applying this method for W-IWM2, effective operation of W-IWM2 and D-WPT can be achieved. Simulations

Table 2: Efficiency measurement on WPT from road to wheel.

Mutual inductance	37.0 μH
Road-side DC input voltage	448.7 V
Wheel-side DC input voltage	451.6 V
Road-side DC input	8.196 kW
Wheel-side DC-link output	7.396 kW
DC to DC transmission efficiency	90.24 %

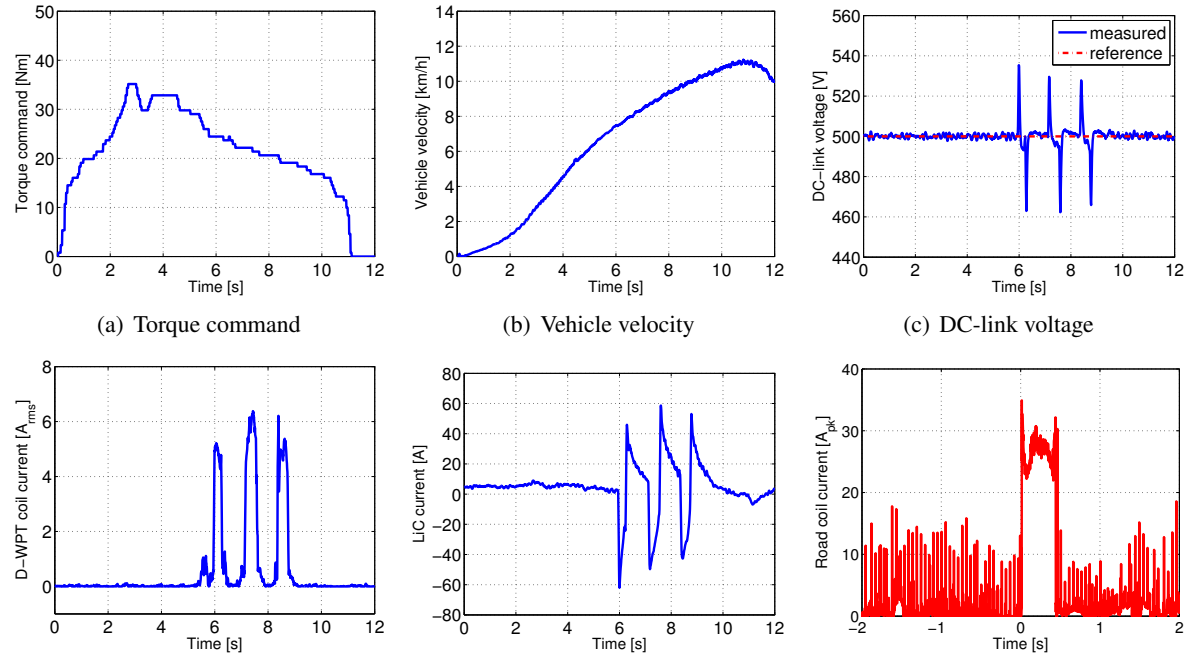

(a) Torque command (b) Vehicle velocity (c) DC-link voltage

(d) The receiving coil for D-WPT current (e) LiC current (f) The road-side coil current

Figure 13: Experimental results of actual vehicle driving test.

and experiments including actual car driving test verified the establishment of the power management method.

ACKNOWLEDGMENT

The research presented in this paper was funded in part by the Ministry of Education, Culture, Sports, Science and technology grant (No. 26249061) and JST CREST Grant Number JPMJCR15K3, Japan. The authors would like to express their deepest appreciation to the Murata Manufacturing Co., Ltd. for providing the laminated ceramic capacitors used in these experiments, Toyo Electric Mfg. Co., Ltd. for offering power converters for W-IWM2, NSK Ltd. for offering reduction gear integrated HUB bearing unit.

References

[1] Atsuo Kawamura, Giuseppe Guidi, Yuki Watanabe, Yukinori Tsuruta, Naoki Motoi and Tae-Woong Kim:“Driving Performance Experimental Analysis of Series Chopper Based EV Power Train”, *Journal of Power Electronics*, Vol.12, No.6, pp.992–1002, (2013).

[2] Yuta Ikezawa, Hiroshi Fujimoto, Yoichi Hori, Daisuke Kawano, Yuichi Goto, Misaki Tsuchimoto and Koji Sato: “Range Extension Autonomous Driving for Electric Vehicles Based on Optimal Vehicle Velocity Trajectory Generation and Front–Rear Driving–Braking Force Distribution with Time Constraint”, *IEEJ Journal of Industry Applications*, Vol.5, No.3, pp.228–235, (2016).

[3] Satoshi Murata: “Innovation by in-wheel-motor drive unit, Vehicle System Dynamics,” *International journal of Vehicle Mechanics and Mobility*, Vol.50, Issue.6, pp.807–830, (2012).

[4] Siqi Li and Chunting Chris Mi: “Wireless Power Transfer for Electric Vehicle Applications,” *IEEE Journal of Emerging and Selected Topics in Power Electronics*, Vol.3, No.1, pp.4–17, (2015).

[5] J. M. Miller, O.C. Onar and M. Chinthavali : “Primary-Side power-flow Control of Wireless Power Transfer for Electric Vehicle Charging,” *IEEE Journal of Emerging and Selected Topics in Power Electronics*, Vol.3, Issue.1, pp.144–162, (2015).

[6] Keisuke Kusaka and Jun-ichi Itou:“Reduction of Reflected Power Loss in an AC-DC Converter for Wireless Power Transfer Systems”, *IEEJ Journal of Industry Applications*, Vol.2, No.4, pp.195–203, (2013).

[7] Motoki Sato, Gaku Yamamoto, Takehiro Imura and Hiroshi Fujimoto:“Experimental Verification of Wireless In-Wheel Motor using Magnetic Resonance Coupling”, *The 9th International Conference on Power Electronics - ECCE Asia*, (2015).

[8] Takuma Takeuchi, Takehiro Imura, Hiroshi Fujimoto, Yoichi Hori, Daisuke Guniji:“Study on Energy System Configuration of Wireless In-Wheel Motor with Supercapacitor”, *The 29th International Electric Vehicle Symposium and Exhibition*, pp. N/A, (2016).

[9] Jian Cao and Ali Emadi: “A New Battery / UltraCapacitor Hybrid Energy Storage System for Electric, Hybrid and Plug-In Hybrid Electric Vehicles,” *IEEE Transaction on Power Electronics*, Vol.27 No.1, pp.122–132, (2012).

[10] Matthew McDonough: “Integration of Inductively Coupled Power Transfer and Hybrid Energy Storage System: A Multiport Power Electronics Interface for Battery-Powered Electric Vehicles,” *IEEE Transaction on Power Electronics*, Vol.30, No.11, pp.6423–6433, (2015).

[11] Dasiuke Gunji, Takehiro Imura, Hiroshi Fujimoto: “Fundamental Research of Power Conversion Circuit Control for Wireless In-Wheel Motor using Magnetic Resonance Coupling”, *40th Annual Conference of the IEEE Industrial Electronics Society* , pp. 3004–3009, (2014).

[12] Daita Kobayashi, Takehiro Imura, Hiroshi Fujimoto and Yoichi Hori: “Sensorless Vehicle Detection Using Voltage Pulses in Dynamic Wireless Power Transfer system,” *Electric Vehicle Symposium & Exhibition 29 – EVS29*, (2016).

Authors

(a)Mr. Takuma Takeuchi received his M.S. degree in electrical engineering from The University of Tokyo, Chiba, Japan in 2017. He is currently working at Toyota Motor Corporation. His research interests are mainly on wireless power transfer via magnetic resonant couplings.
(b)Dr. Takehiro Imura received his B.S. degree in electrical and electronics engineering from Sophia University, Tokyo, Japan. He received his M.S. degree and Ph.D. in Electronic Engineering from The University of Tokyo in March 2007 and March 2010 respectively. He is currently a Specially Appointed Associate in the Graduate School of Engineering in the same university.
(c)Dr. Hiroshi Fujimoto received his Ph.D. in electrical engineering from The University if Tokyo in 2001. In 2001, he joined the Department of Electrical and Computer Engineering, Nagaoka University as a research associate. From 2002 to 2003, he was a visiting scholar in the School of Mechanical Engineering, Purdue University. In 2004, he joined the Department of Electrical and Computer Engineering, Yokohama National University as a lecturer and he became an associate professor in 2005. He is currently an associate professor of the University of Tokyo since 2010.
(d)Dr. Yoichi Hori received his Ph.D. in electrical engineering from The University of Tokyo, Japan, 1983, where he became a Professor in 2000. In 2008, he moved to the Department of Advanced Energy, Graduate School of Frontier Sciences. Prof. Hori was the recipient of the Best Paper Award from the IEEE Transactions on Industrial Electronics in 1993, 2001 and 2013 and of the 2000 Best Paper Award from the Institute of Electrical Engineers of Japan (IEEJ). He is the Chairman of the Motor Technology Symposium of the Japan Management Association.


(a)


(b)


(c)


(d)